Supplement material for the paper

Long-term aerosol optical hygroscopicity study at the ACTRIS SIRTA observatory: synergy between ceilometer and in-situ measurements

Andrés Esteban Bedoya-Velásquez [1,2,3], Gloria Titos [1,2,4], Juan Antonio Bravo-Aranda [1,2], Martial Haeffelin[5], Olivier Favez[6], Jean-Eudes Petit[7], Juan Andrés Casquero-Vera[1,2], Francisco José Olmo-Reyes[1,2], Elena Montilla-Rosero[8], Carlos D. Hoyos[9], Lucas Alados-Arboledas [1,2] and Juan Luis Guerrero- Rascado [1,2].

1 Effect of beta-attenuated water vapor correction on calculated $f_{\beta}(RH)$ and γ parameter

The β^{att} signal presents a dependency on water vapor absorption as shown in Sec. 3.1 (Eq.8), associated with the wavelength emission. This dependency may cause direct effects over calculations retrieved by using β^{att}. Here, we present the correction applied to β^{att} and the effects on $f_{\beta}(RH)$ and γ calculations. Figure S1 (left-panels) represents the temporal-evolution of β^{att}, beta attenuated water vapor corrected (β^{att}_{wv}) signals over 3 h time-window, together with the temporal-evolution of q. . Figure S1 (right-panels) shows the biases for beta ($bias_{\beta}$) and Δ_q obtained.

The quantifications are performed by means of the $bias_{\beta}$ ($\beta^{att} - \beta^{att}_{wv}$) and Δ_q $\left(q(t) - q\ (t_d)\right)$ calculations. Fig. S1ac presents two cases (case 1 and case 2) with low absolute-differences in q, which produces slight changes in β^{att}_{wv} signal respect to β^{att}. On the other hand, Fig. S1eg (case 3 and case 4) show that high absolute-differences in q are linked to high changes on β^{att}_{wv}. The right side of the panel (Fig. 1Sbd, case 1 and case 2), presents the bias quantification, showing that low $bias_{\beta}$ are associated with low Δ_q and, on the contrary, Fig. 1Sfh (case 3 and case 4), show that increases in Δ_q makes that $bias_{\beta}$ becomes higher. This analysis leads us to conclude that no-water vapor correction will produce an overestimation of the total β signal, being $\Delta_q$the parameter that rules the β correction. From now, we will use β instead of β^{att} for simplicity.

To see the effect of β^{att}_{wv} on $f_{\beta}(RH)$, we applied the Hänel parameterization (Eq. 7, Sec. 3.1 of the manuscript) to the same 4 cases studied above. Figure S2 presents the $f_{\beta}(RH)$ and the enhancement factor water vapor corrected, $f_{\beta^{att}_{wv}}(RH)$. The results reinforce those obtained above (Fig S1), where low/high changes in Δ_q are linked with low/high $bias_{\beta}$ and, on this way, this would affect $f_{\beta}(RH)$ calculation. Additionally, the water vapor correction tends to decrease γ (β^{att}_{wv} is lower than β). Therefore, cases with lower $bias_{\beta}$ and Δ_q (case 1 and case 2), exhibits lower $bias_{\gamma}$ (0.02 and 0.05, respectively), meanwhile on case 3 and case 4 instead $bias_{\beta}$ increase, the $bias_{\gamma}$ becomes higher (0.11 and 0.09, respectively).

Once we applied the phase 2 of the methodology (Sec. 5), we obtain 94 hygroscopic potential cases for 3h time-window (Fig. S3a), 9 cases for 4h time-window (Fig. S3a) and 4 cases for 5h time-window (Fig. S3a), resulting in a total of 107 cases. To establish a bias error for this hygroscopic study, we have calculated the median of the bias$_\beta$ and Δ_q, highlighting two main aspects: (i) The median bias$_\beta$ follows the median Δ_q variability, remarking their dependency. This fact is well seen from the scatter plot (Fig. 3Sb), where these variables show a positive correlation, however the correlation coefficient is not too high (R^2= 0.61), mainly because the data dispersion increases for bias$_\beta$ > 1.5 10^{-7} $m^{-1}\cdot sr^{-1}$ and Δ_q > 3.0 g/m^3; (ii) The mean bias error calculated for β_{wv}^{att} over the 107 potential cases evaluated is lower than $2.5\cdot10^{-7}$ $m^{-1}\cdot sr^{-1}$ and the mean Δ_q is lower than 5.5 g/m^3.

Fig. S4 quantifies the effect of the β_{wv}^{att} over $f_\beta(RH)$ and γ hygroscopic properties, by means of the median bias$_{f_\beta(RH)}$ ($f_\beta(RH)$ - $f_{\beta_{wv}^{att}}(RH)$) and the bias $_\gamma$ ($\gamma_{\beta^{att}} - \gamma_{\beta_{wv}^{att}}$). Figure S4 reveals the no-correlation between bias$_\beta$ and bias$_{f_\beta(RH)}$. However, combining the results from Fig. S3 and Fig. S4, it is possible to establish that bias$_\beta$ > 1 $m^{-1}\cdot sr^{-1}$ would cause an increment of bias$_{f_\beta(RH)}$ above 0.2, increasing the error on $f_\beta(RH)$. Finally, it was obtained that bias$_{f_\beta(RH)}$ and bias $_\gamma$ for the whole study were lower than 0.3.

2 Results

2.1 Methodology applied to eight aerosol hygroscopic growth cases

The 8 hygroscopic growth cases reported in this study (Table 1, Sec. 5.2) were found at daytime in the early morning, with RH_{ref} around 50 % and the maximum RH reached was up to 90% over 3h time-window. For cases 1, 2, 4, 5, 6 and 7 the perceptual composition was dominated by OA with values up to 50 %, except on case 7 where OA decreased up to 38%. The BC concentration was relatively low almost for all cases found (close to 6 %). The concentration of inorganic compounds were dominated by SO_4^{2-} (lower than 21 %) and NH_4^+(lower than 19 %), however NO_3^- reached values of 21% on case 6. The air masses that come mainly from W-NW direction are related to case 1 (Δu=3.6 m/s W), case 2 (Δu=23.0 m/s NW) and case 6 (Δu=4.4 m/s W), with speed variability up to 14.2 %, 20.7 % and 18.5 %, respectively; and the air masses that coming from W-SW direction at low wind direction variability are associated with case 4 (Δu=2.7 m/s W), case 5 (Δu=2.4 m/s SW), and case 7 (Δu=1.7 m/s SW), and wind speed variability about 15.4 m/s, 20.4 m/s and 10.9 m/s, respectively. All these cases fulfilled the threshold established for $\frac{\Delta f_{PM1}(RH)}{\Delta f_\beta(RH)} < 0.5$ indicating that increases/decreases in $f_\beta(RH)$ are not related with advected aerosol into the atmospheric volume studied. The Hänel parameterization is calculated for both $f_\beta(RH)$ and $f_{PM1}(RH)$ (see panel Fig. S4 to S9 b.). The hygroscopicity properties of the 6 cases presented here were evaluated and compared against literature in the Sec. 5.2 of the article.

Figures

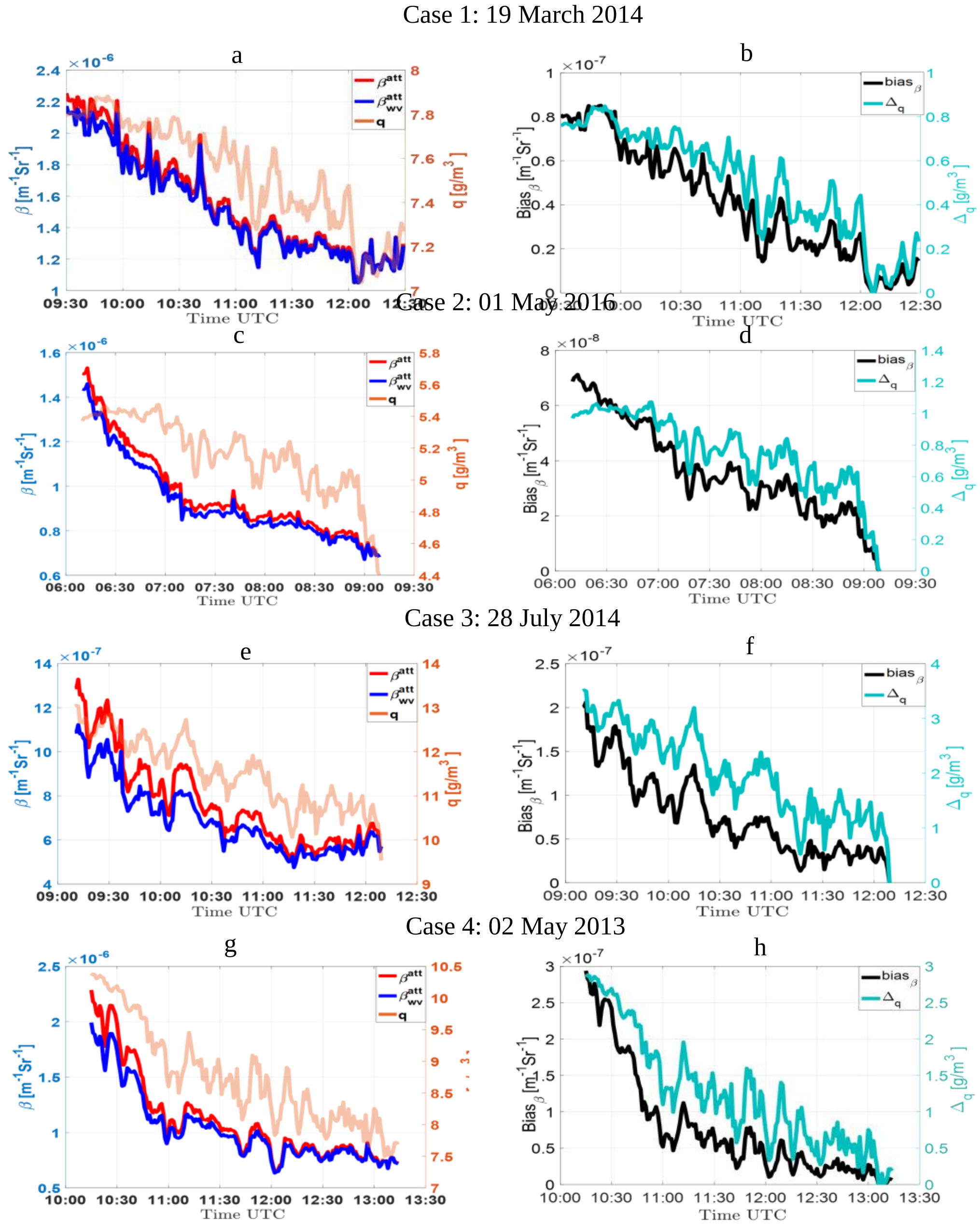

Figure S1. Time evolution of β^{att}(blue line), β_c^{att}(red line) and q (orange line)[left panels (a,c,e,g $bias_\beta$ (black line) and Δ_q (green line) [right panel (b,d,f,h)].

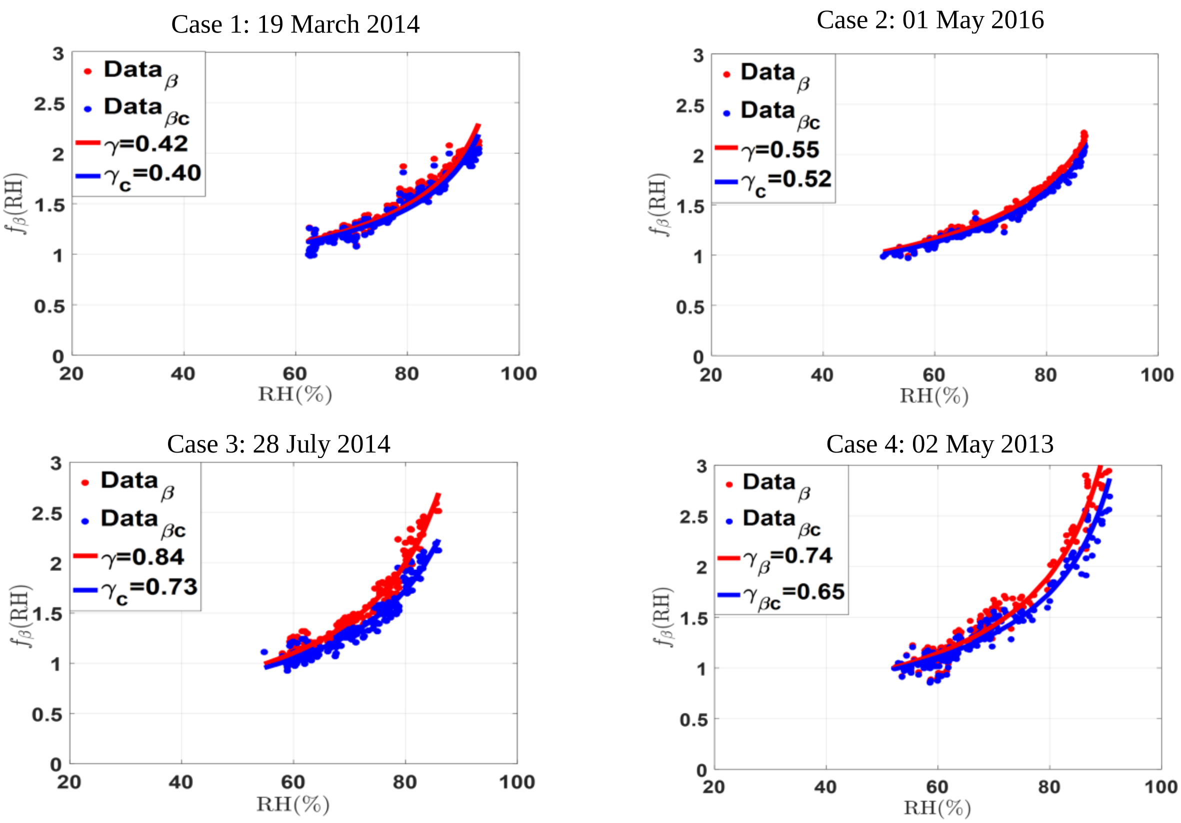

Figure S2. Experimental data points (blue/red dots) and Hänel parameterization (blue/red lines). Case 1 and Case 2 show the effect of the lower bias$_\beta$ and Δ_q differences over $f_{\beta_{wv}^{att}}(RH)$ and $f_\beta(RH)$. Case 3 and Case 4 present the effect of the higher bias$_\beta$ and Δ_q differences over $f_{\beta_{wv}^{att}}(RH)$ and $f_\beta(RH)$.

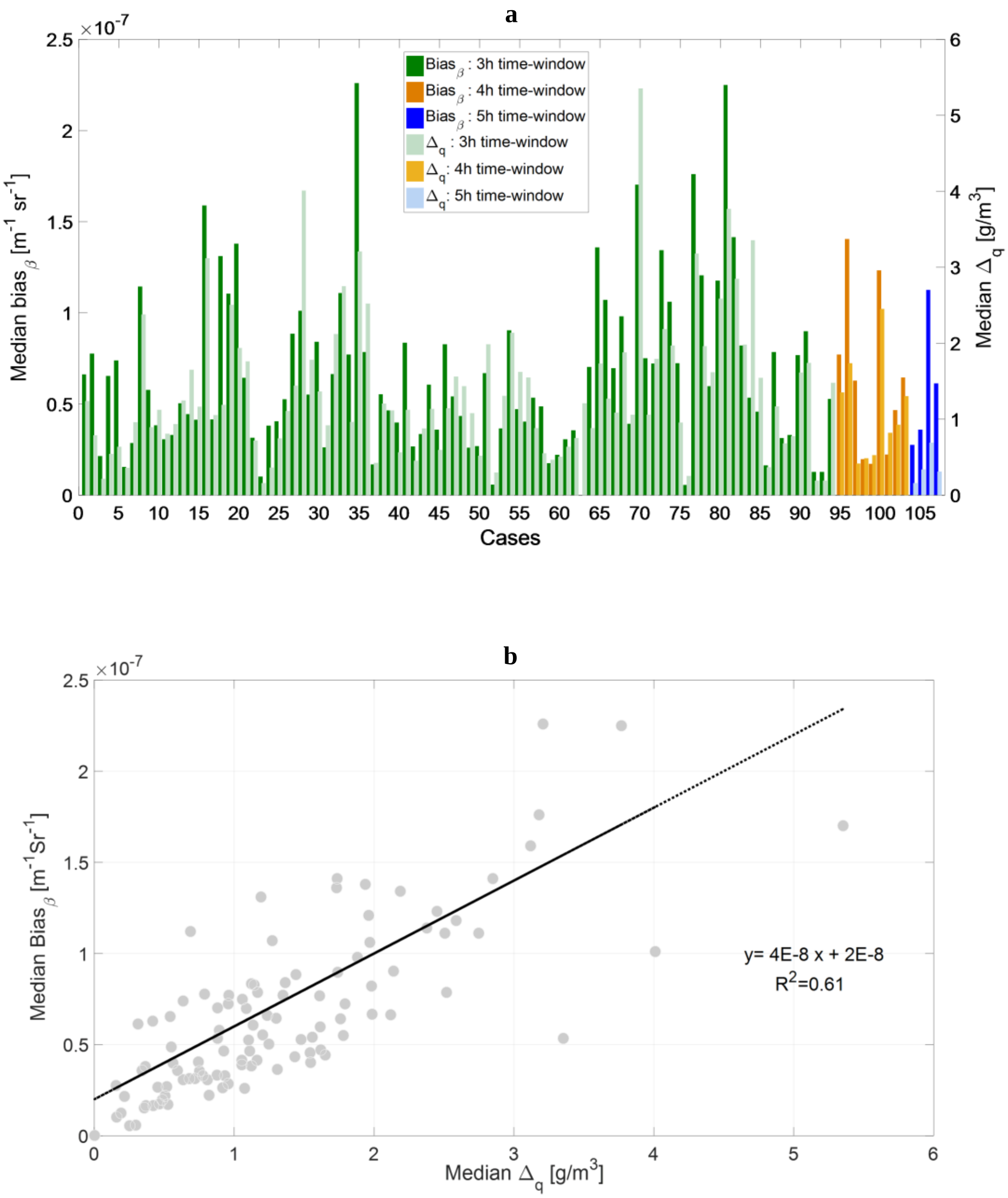

Figure S3. Median of bias$_\beta$ and Δ_q for all potential cases of hygroscopic growth found from 2012 to 2016 at the ACTRS SIRTA observatory: (a median of bias$_\beta$ and Δ_q to 3h time-window analysis (green bars), 4h time-window analysis (orange bars) and 5h time-window analysis (blue bars); (b) scatter plot correlating median of bias$_\beta$ and Δ_q for whole time-windows.

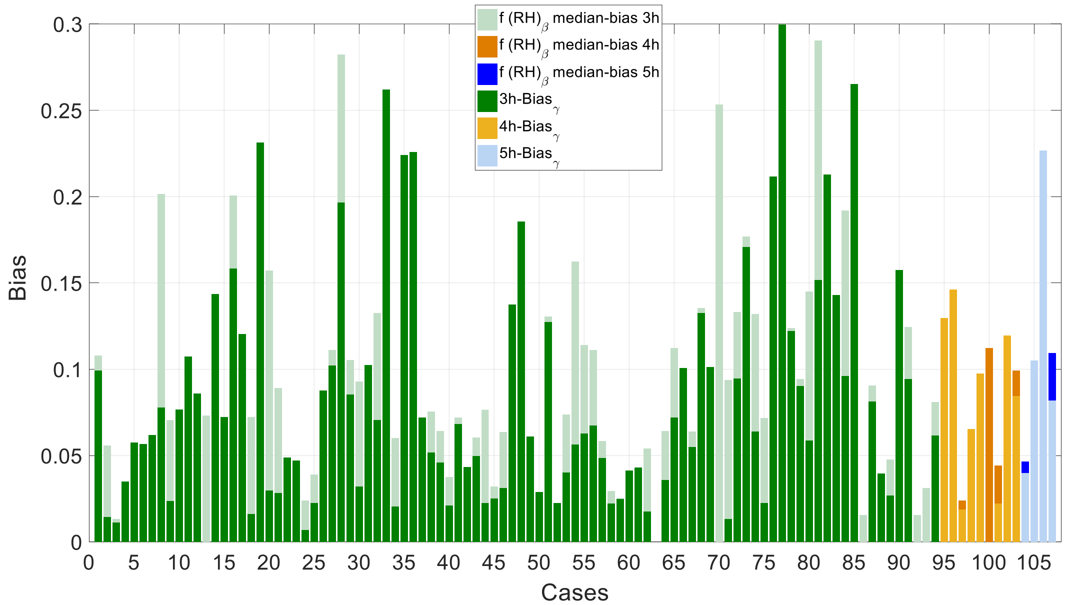

Figure S4. $\text{bias}_{f_{\beta}(RH)}$ and $bias_{\ \gamma}$ for all potential cases of hygroscopic growth found from 2012 to 2016 at the ACTRIS SIRTA observatory. $\text{bias}_{f_{\beta}(RH)}$ and bias $_{\gamma}$ for 3h time-window analysis (green bars), 4h time-window analysis (orange bars) and 5h time-window analysis (blue bars).

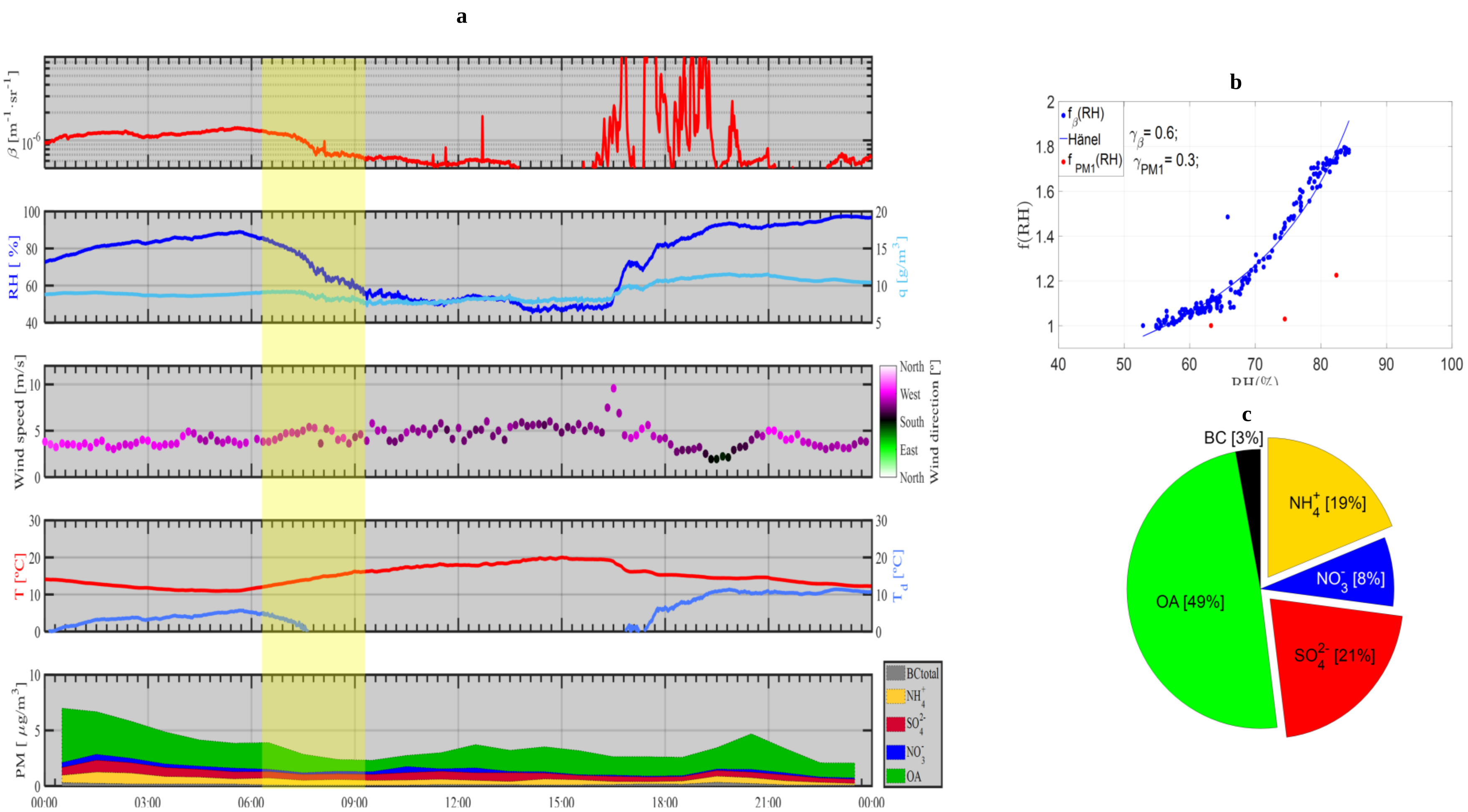

Figure S5. Criterion for data selection: case 1 on 29 July 2012 from 06:30 to 09:30 UTC.

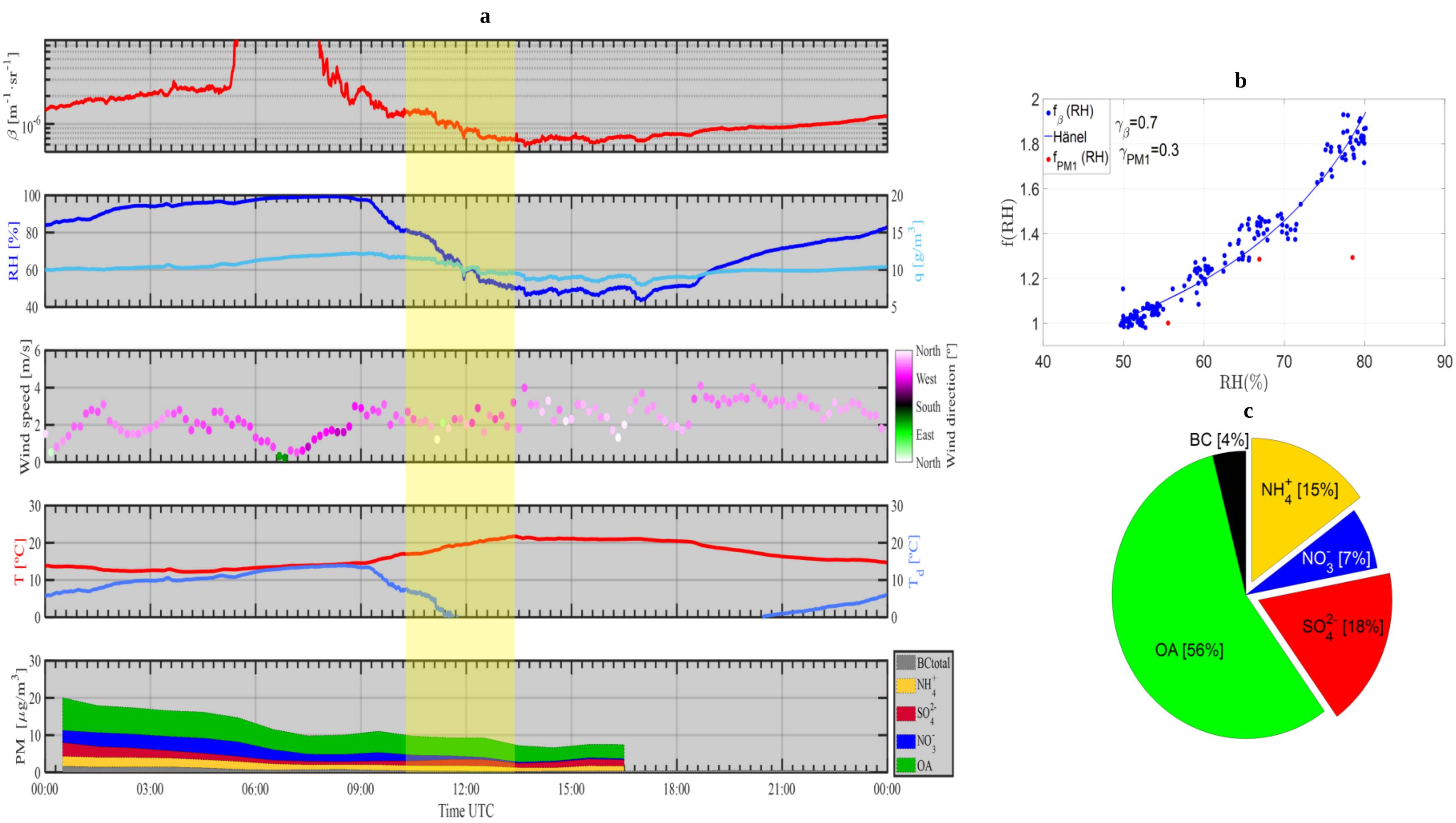

Figure S6. Criterion for data selection: case 2 on 02 September 2012 from 10:30 to 13:30 UTC.

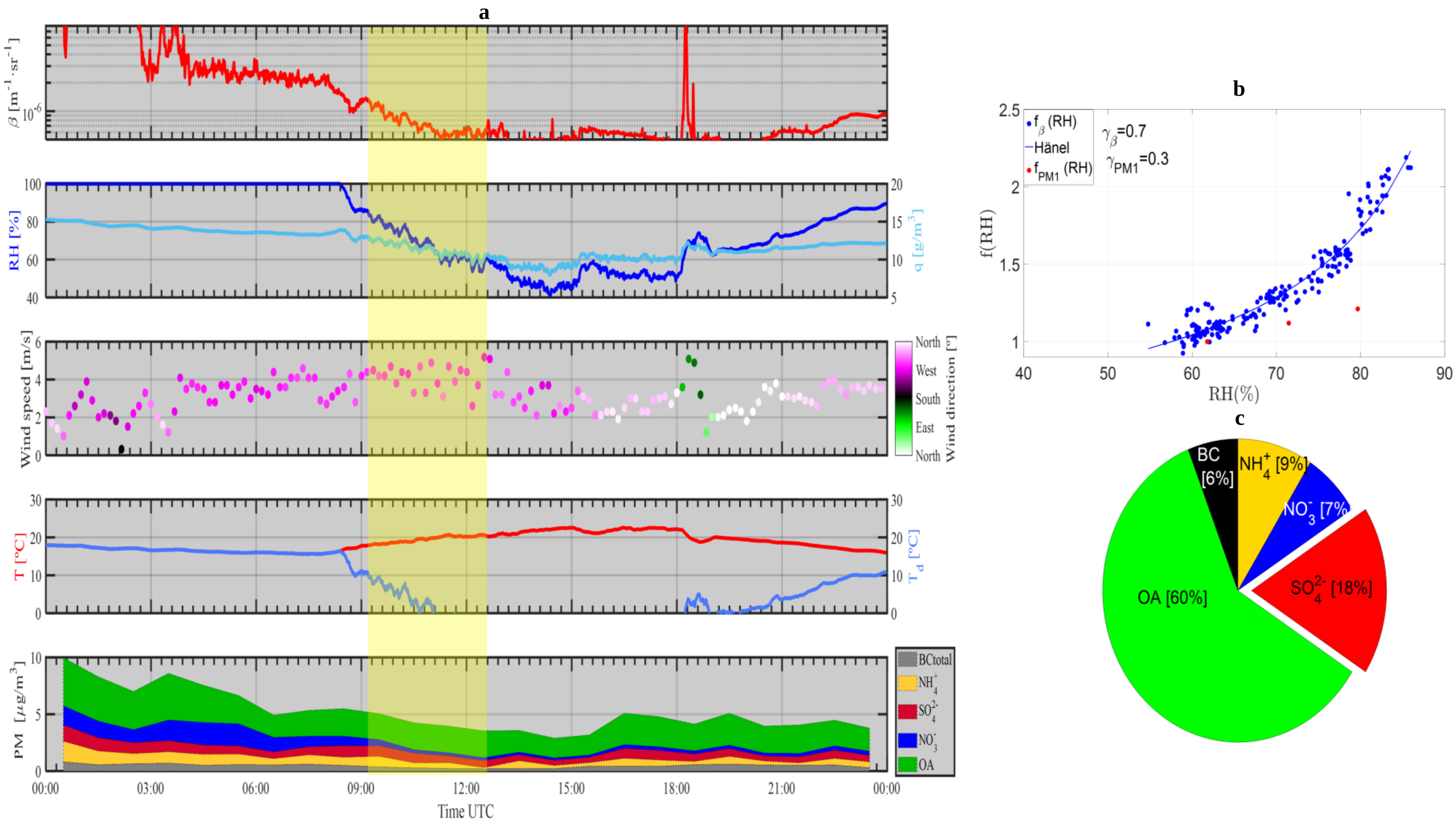

Figure S7. Criterion for data selection: case 4 on 28 July 2014 from 09:10 to 12:10 UTC.

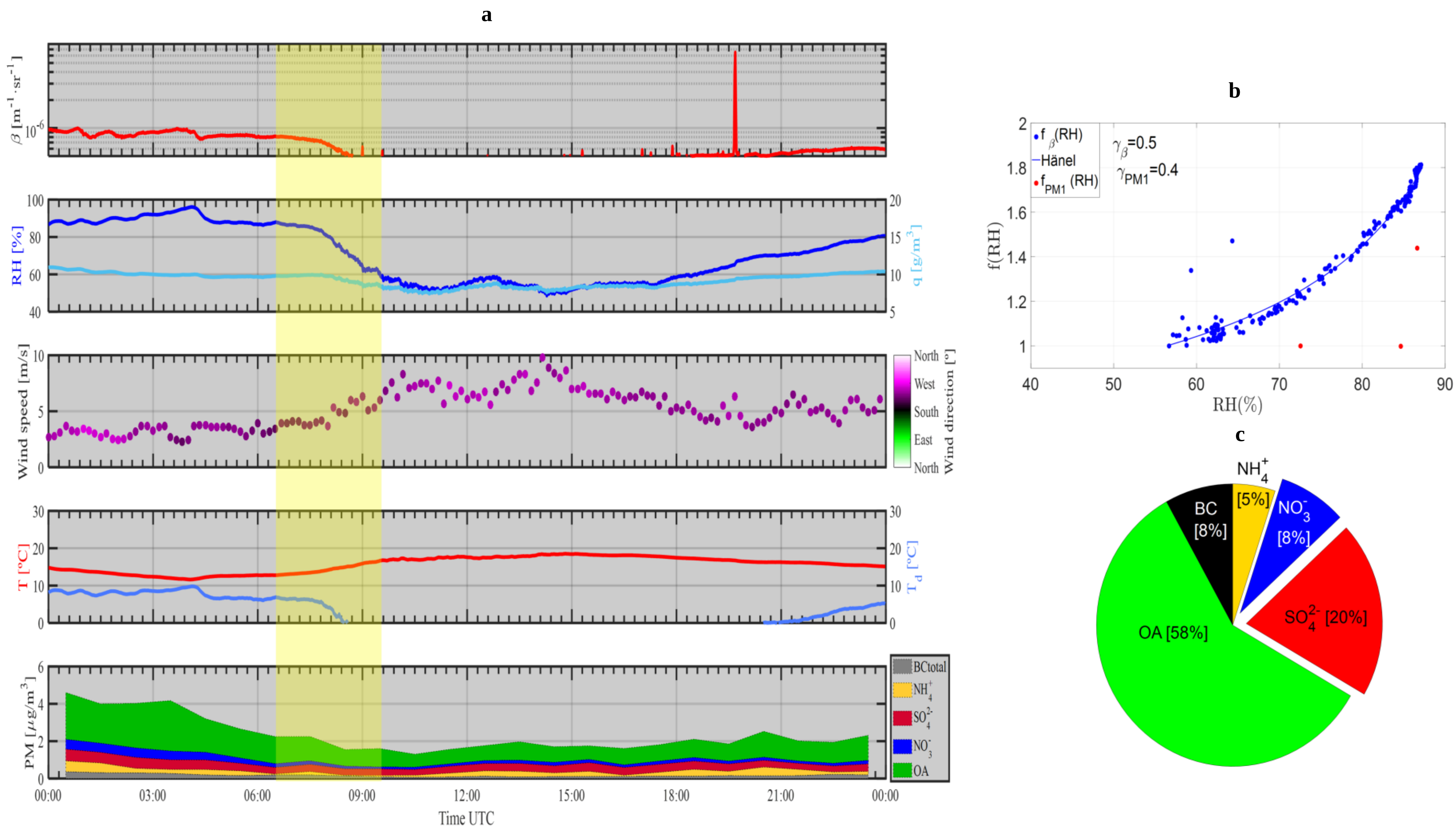

Figure S8. Criterion for data selection: case 5 on 17 August 2014 from 06:40 to 09:40 UTC.

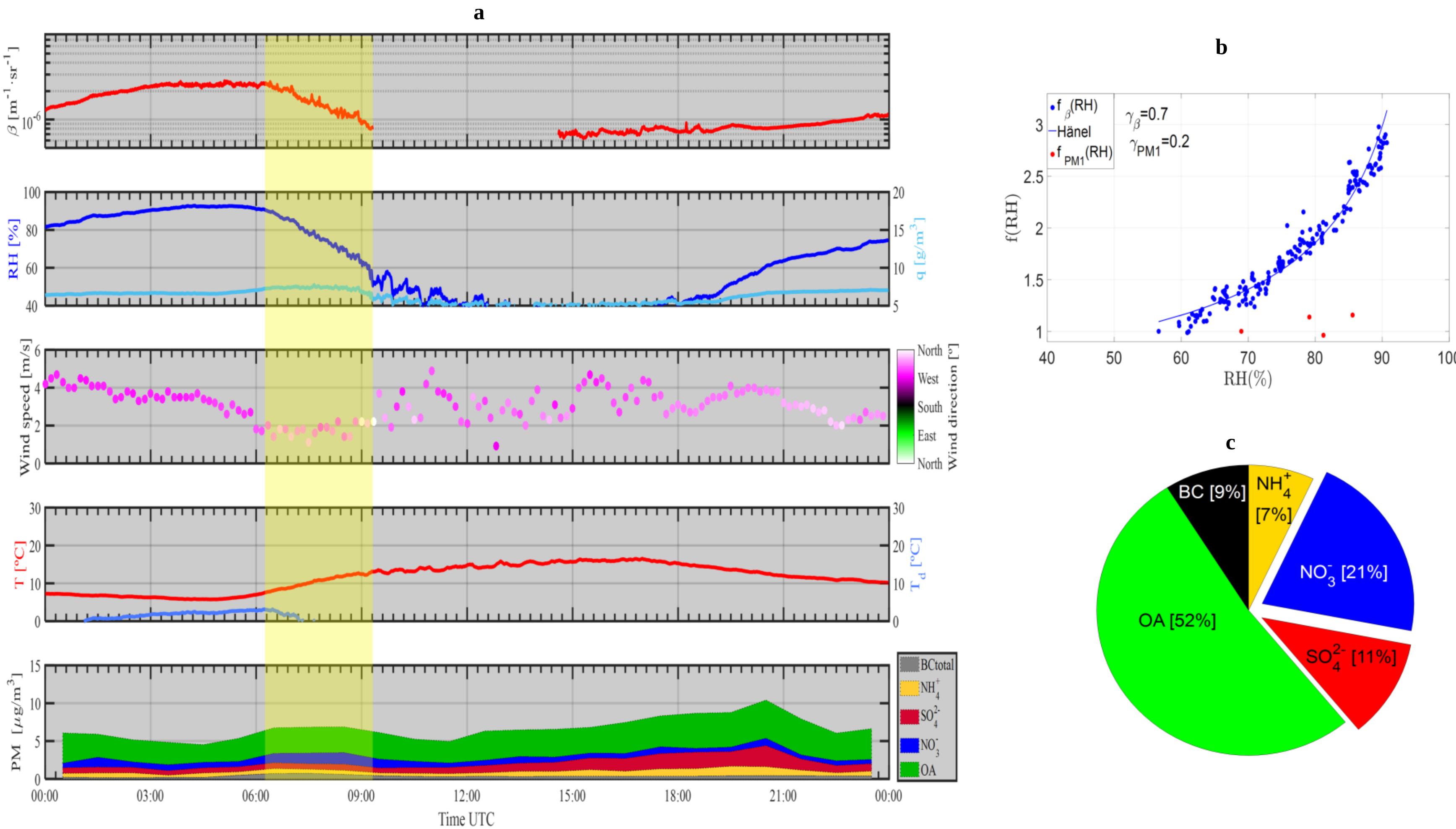

Figure S9. Criterion for data selection: case 6 on 21 May 2015 from 06:15 to 09:15 UTC.

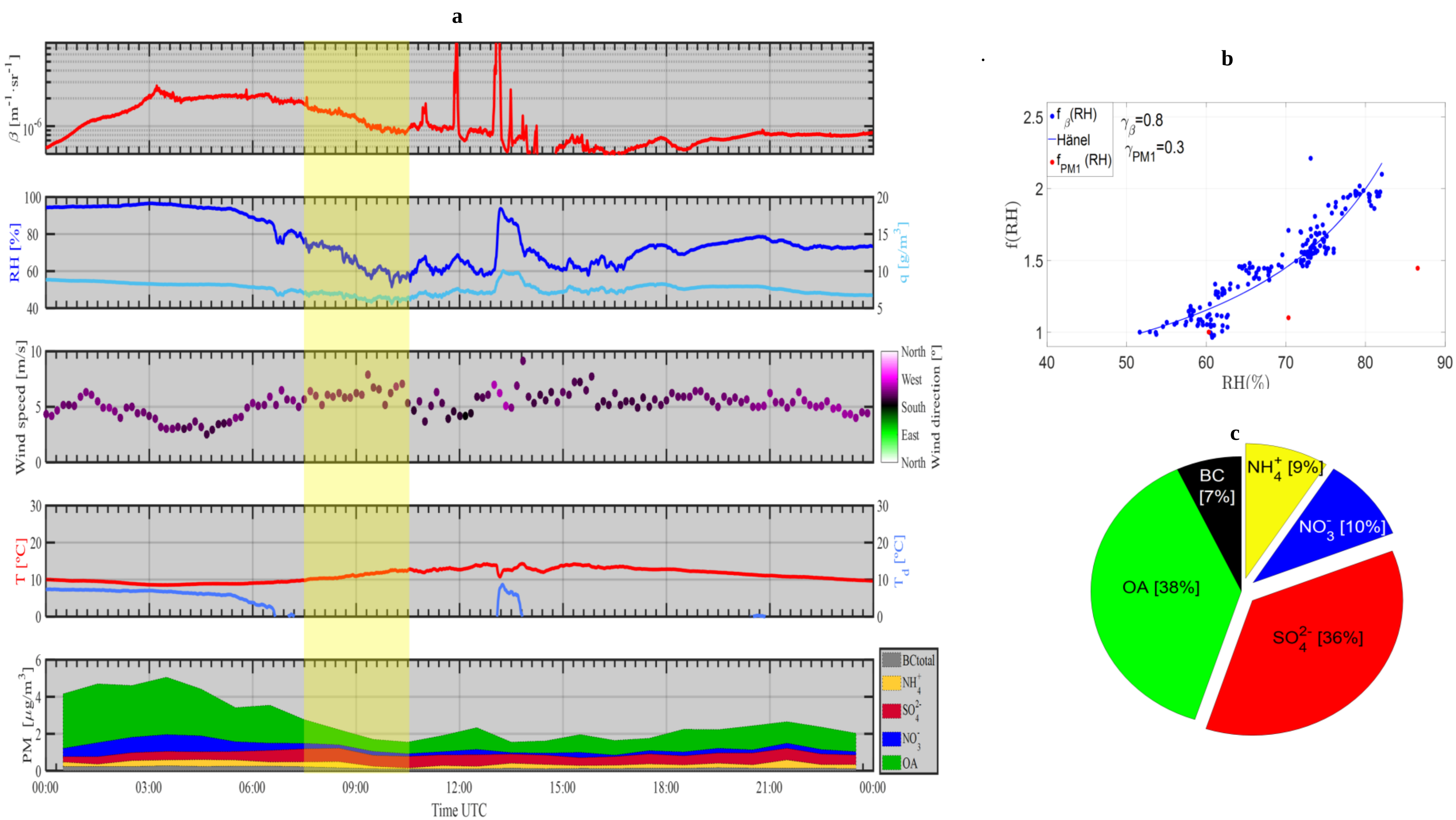

Figure S10. Criterion for data selection: case 7 on 15 April 2016 from 07:05 to 10:05 UTC.